www.sphinxsai.com

ChemTech

International Journal of ChemTech Research
CODEN (USA): IJCRGG ISSN : 0974-4290
Vol.6, No.14, pp 5466-5475, Nov-Dec 2014

DFT investigation on structural stability and electronic properties of α-Si_3N_4 and β-Si_3N_4 nanostructures

V. Nagarajan, V. Saravanakannan, R. Chandiramouli*

School of Electrical & Electronics Engineering
SASTRA University, Tirumalaisamudram, Thanjavur -613 401, India

***Corres.author : rcmoulii@gmail.com, Tel: +919489566466**
Fax.:+91-4362-264120

Abstract : The realistic pure, Ge and O substituted Si_3N_4 nanostructures are optimized and simulated successfully using B3LYP/LanL2DZ basis set. Structural stability and electronic properties of α-Si_3N_4 and β-Si_3N_4 nanostructures are studied in terms of calculated energy, electron affinity, HOMO – LUMO gap and ionization potential. Dipole moment and point symmetry group of silicon nitride nanostructures are also reported. The stable nanostructures of silicon nitride are discussed with the help of substitution impurity. The structural stability & electronic properties can be fine-tuned with impurity substitution and creating defects in nanostructure which find its potential importance in cutting tools, engine components and microelectronic devices.
Keywords: silicon nitride; ionization potential; point group; dipole moment; electron affinity.

Introduction

Silicon nitride (Si_3N_4) is an important ceramic material owing to its mechanical, chemical and electronic properties; it has been used in cutting tools, engine components and microelectronic devices due to its excellent mechanical properties. Si_3N_4 is chemically inert and has a wide-band gap with high dielectric constant [1-3]. The other significant property of Si_3N_4 is good resistance to oxidation, high hardness, corrosion, high mechanical strength and thermal shock [4-8].

There are many methods in the synthesis of Si_3N_4 such as direct nitridation, nitridation of SiO_2 and carbothermal reduction, chemical vapor phase technique, self-propagation combustion at high-temperature and thermal decomposition of $Si(NH)_2$ [9-12]. The experimental and theoretical electronic band gap of Si_3N_4 is around 5.1 -5.3 eV [13-15] and 6.7 eV [16] respectively. In the past two decades, Si_3N_4 thin films are synthesized and studied as a passivation layer for silicon solar cells and antireflection coatings [17-22]. The quality and properties of these films are influenced by their stoichiometry and structure, which are primarily dependent on deposition technique such as pressure, gas-phase composition and temperature [23]. The optimized crystal structure of Si_3N_4 has been reported [24-26]. Many works are reported by authors who mainly concentrated in nitridation of Si (111) surfaces and Si (100) surfaces [27, 28].

In this work, both α-Si_3N_4 and β-Si_3N_4 nanostructures are optimized and simulated successfully using density functional theory (DFT) [29-31]. The substitution of impurities such as oxygen and germanium are incorporated in pure silicon nitride nanostructure to enhance the structural stability and electronic properties of Si_3N_4 nanostructures.

Computational details

The pure structure and O & Ge substituted α-Si_3N_4 and β-Si_3N_4 nanostructures are optimized successfully with Gaussian 09 package [32]. The present work explores the structural stability and electronic

properties of silicon nitride. The nanostructures of Si_3N_4 are optimized by Becke's three-parameter hybrid functional in combination with Lee-Yang-Parr correlation functional (B3LYP) and LanL2DZ basis set. For optimization of Si_3N_4 nanostructures, LanL2DZ is the appropriate basis set, since it is applicable to the elements such as H, Li-La and Hf-Bi [33, 34]. Gauss Sum 3.0 [35] is used to determine HOMO – LUMO gap and DOS spectrum of Si_3N_4 nanostructures.

Results and discussion

The present work primarily focuses on dipole moment (DM), electron affinity (EA), HOMO – LUMO gap, calculated energy, ionization potential (IP) and point group (PG) of pure, O and Ge substituted α-Si_3N_4 and β-Si_3N_4 nanostructures. Figure 1 (a) – Figure 1 (c) represents pure, O and Ge substituted α-Si_3N_4 nanostructures respectively. In that order, pure Si_3N_4 nanostructures has thirteen N atoms and eleven Si atoms to form a mesh like structure, O substituted α-Si_3N_4 nanostructures consists of eleven Si atoms; eleven N atoms and two N atoms are replaced with two O atoms followed by Ge substituted α-Si_3N_4 nanostructures which contains thirteen N atoms, ten Si atoms and one Si atom are replaced with one Ge atom. Figure 1 (d) illustrates the defect structured α-Si_3N_4 nanostructure with the removal of two N atoms and one Si atom in pure α-Si_3N_4 nanostructures. Figure 1 (e) – Figure 1 (g) denotes pure, O and Ge substituted β-Si_3N_4 nanostructures. The pure β-Si_3N_4 nanostructure has twelve N atoms and twelve Si atoms to form tube-like structure. O substituted β-Si_3N_4 nanostructure consists of ten N atoms; twelve Si atoms and two N atoms are replaced with two O atoms. Ge substituted β-Si_3N_4 nanostructure contains twelve N atoms; eleven Si atoms and one Si atom are replaced with one Ge atom. Figure 1 (h) represents a defect structured β-Si_3N_4 nanostructure in which two N atoms and one Si atom are removed.

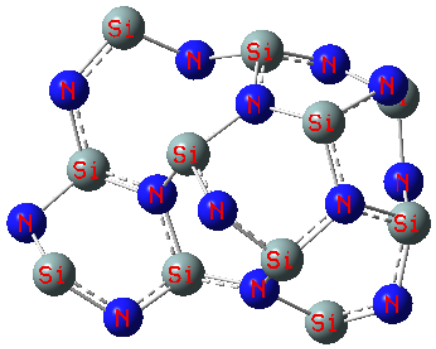

Figure. 1(a) Structure of pure α-Si_3N_4 nanostructure

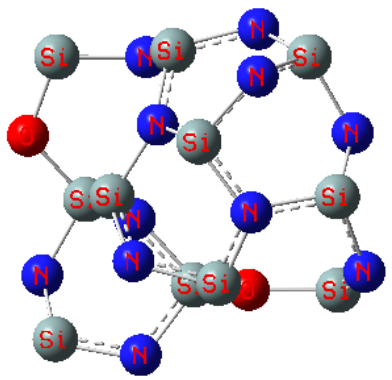

Figure. 1(b) Structure of O substituted α-Si_3N_4 nanostructure

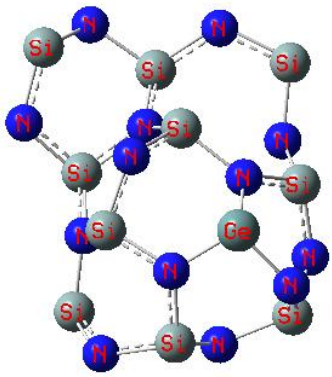

Figure. 1(c) Structure of Ge substituted α-Si_3N_4 nanostructure

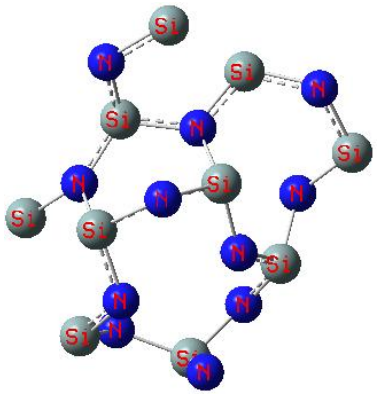

Figure. 1(d) Defect structured α-Si_3N_4 nanostructure

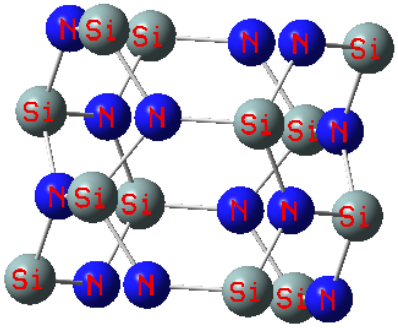

Figure. 1(e) Structure of pure β-Si_3N_4 nanostructure

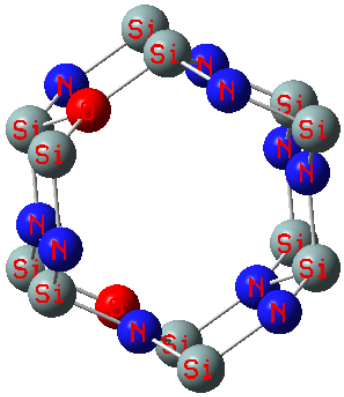

Figure. 1(f) Structure of O substituted β-Si_3N_4 nanostructure

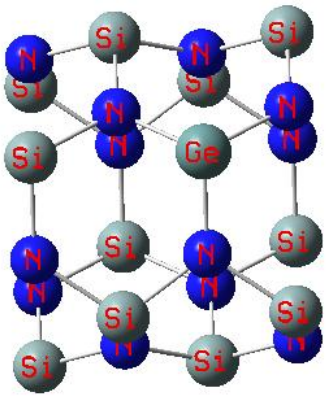

Figure. 1(g) Structure of Ge substituted β-Si_3N_4 nanostructure

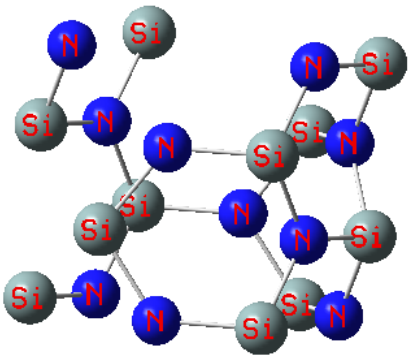

Figure. 1(h) Defect structured β-Si_3N_4 nanostructure

In this work, the structural stability of both α-Si_3N_4 and β-Si_3N_4 nanostructures are discussed through calculated energy. Table 1 displays calculated energy, point group and dipole moment of Si_3N_4 nanostructures.

Table. 1 Energy, point symmetry and dipole moment of silicon nitride nanostructures

Nanostructures	Energy (Hartrees)	Dipole moment (Debye)	Point Group
Pure α-Si_3N_4 nanostructure	-748.45	11.12	C_1
O substituted α-Si_3N_4 nanostructure	-789.4	7.49	C_1
Ge substituted α-Si_3N_4 nanostructure	-748.37	12.21	C_1
Defect structured α-Si_3N_4 nanostructure	-635.67	11.09	C_1
pure β-Si_3N_4 nanostructure	-697.89	0.001	C_1
O substituted β-Si_3N_4 nanostructure	-738.78	6.88	C_1
Ge substituted β-Si_3N_4 nanostructure	-697.77	0.31	C_1
Defect structured β-Si_3N_4 nanostructure	-585.06	13.66	C_1

The calculated energy of pure, O and Ge substituted α-Si_3N_4 nanostructures are -748.45, -789.4 and -748.37 Hartrees respectively. In that order calculated energy of pure, O and Ge substituted β-Si_3N_4 nanostructures are -697.89, -738.78 and -697.77 Hartrees respectively. It implies that one way to increase structural stability of silicon nitride is by substituting the acceptable amount of O atoms. In contrast, the structural stability of defect structured Si_3N_4 nanostructures decreases owing to removal of atoms from regular

structure. Interestingly, the calculated energy for both pure and Ge substituted Si_3N_4 have the same energy, only the change is noticed in the fractional part. Dipole moment gives the perception of the uniform charge distribution along Si_3N_4 nanostructures. Compared to α-Si_3N_4, β-Si_3N_4 nanostructures have a low dipole moment. It shows that the atoms are perfectly arranged in a regular manner and uniform charge distribution is seen in β-Si_3N_4 nanostructures rather than α-Si_3N_4 and defect structured Si_3N_4 nanostructures. The pure, O, Ge substituted α-Si_3N_4 and defect structured α-Si_3N_4 nanostructures have the corresponding DM of 11.12, 7.49, 12.21 and 11.09 Debye respectively. Similarly, in that order, β-Si_3N_4 nanostructures have the DM value of 0.001, 6.88, 0.31 and 13.66 Debye. C_1 point symmetry is observed for all Si_3N_4 nanostructures which have one symmetry operation, identity operation E.

Density of states and HOMO-LUMO gap of Si_3N_4 nanostructures

The electronic properties of Si_3N_4 nanostructures can be examined in terms of highest occupied molecular orbital (HOMO) and lowest unoccupied molecular orbital (LUMO) [36, 37]. The energy gap value for pure β-Si_3N_4 nanostructures has 6.19 eV. This infers the electrons in the valence band needs more energy to transit towards the conduction band. However, the HOMO – LUMO gap of Si_3N_4 nanostructures can be fine-tuned with the help of substituting acceptable impurities such as O and Ge element. The energy gap values for O and Ge substituted β-Si_3N_4 nanostructures have 3.01 and 6.17 eV respectively. It is observed that the gap between the valence band and the conduction band is comparatively low with pure β-Si_3N_4 nanostructures. Defect structured β-Si_3N_4 nanostructure HOMO – LUMO gap value is 3.82 eV, which are lower than pure β-Si_3N_4 nanostructures. The creation of defect at the particular site in β-Si_3N_4 will also change the band gap. From this, it inferred that the position of the defect also plays a vital role in decreasing the HOMO – LUMO gap.

In α-Si_3N_4 nanostructures, both alpha and beta gap arise due to up spin and down spin of electrons. The band gap value of pure, O and Ge substituted α-Si_3N_4 nanostructure with spin up alpha gaps are 5.09, 5.39 and 5.27 eV respectively. Likewise, for spin down beta band gap values are 5.04, 5.21 and 4.71 eV respectively. These low-energy gaps are highly reactive in chemical reactions. Table 2 shows visualization of HOMO – LUMO gap and density of states (DOS).

Table. 2 HOMO-LUMO gap and density of states of Si_3N_4 nanostructures

Nano structures	**HOMO – LUMO Visualization** HOMO LUMO	**E_g (eV)**	**HOMO, LUMO and DOS Spectrum**
Pure α-Si_3N_4 nanostructure	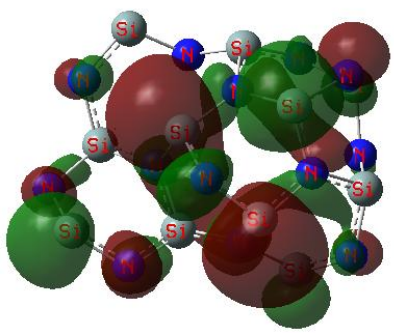	5.04	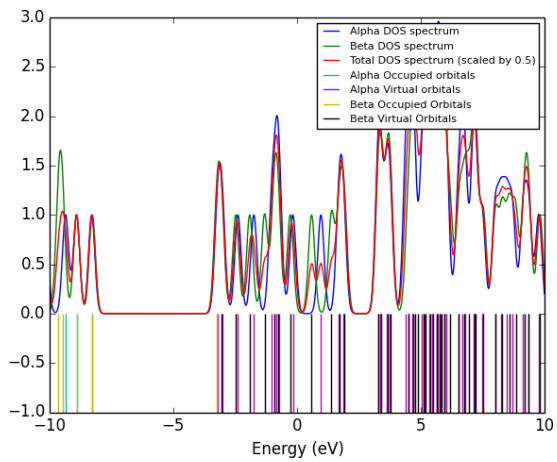

O substituted α-Si_3N_4 nanostructure	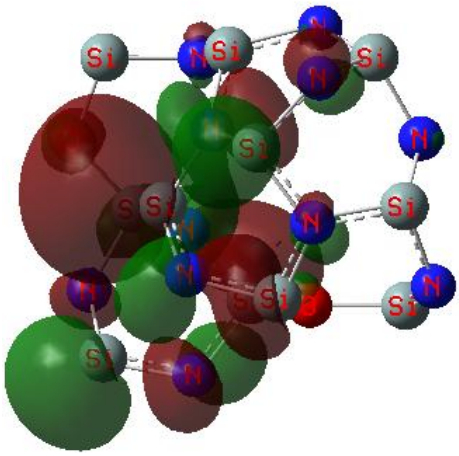	5.21	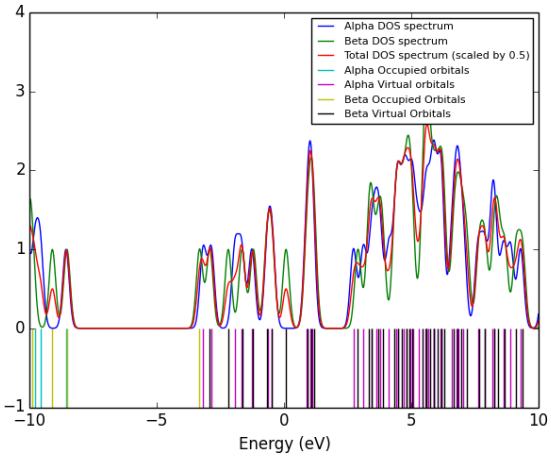
Ge substituted α-Si_3N_4 nanostructure	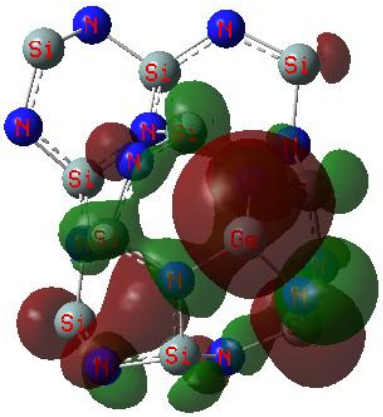	4.71	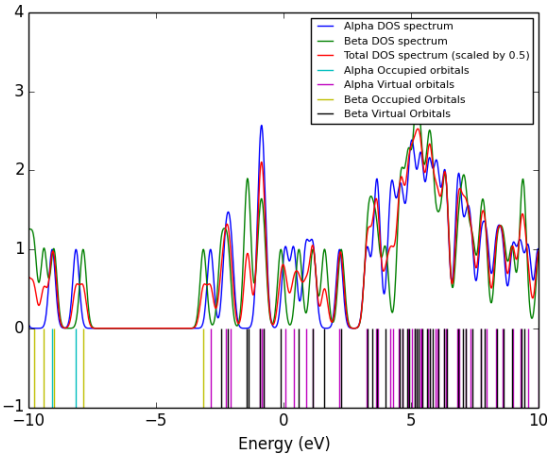
Defect structured α-Si_3N_4 nanostructure	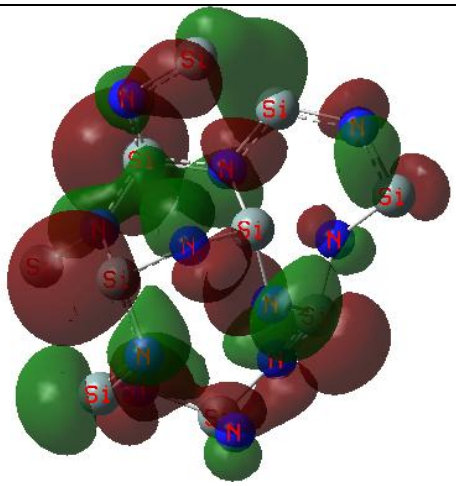	3.54	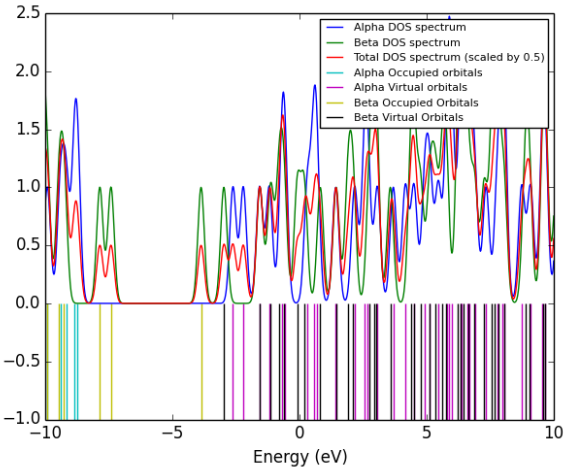

pure β-Si_3N_4 nanostructure	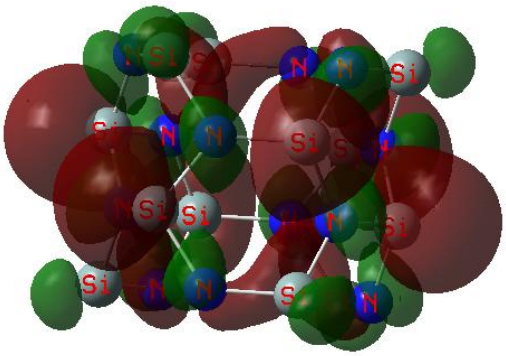	6.19	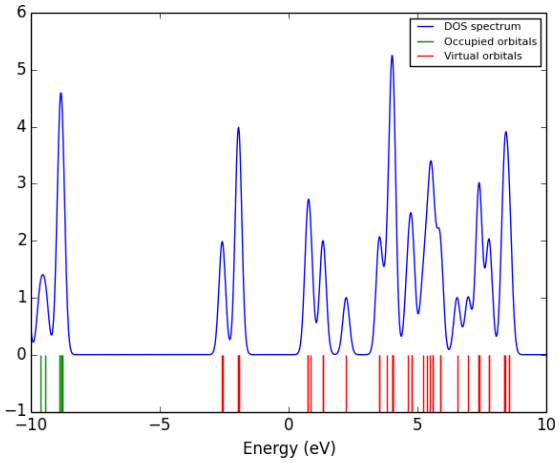
O substituted β-Si_3N_4 nanostructure	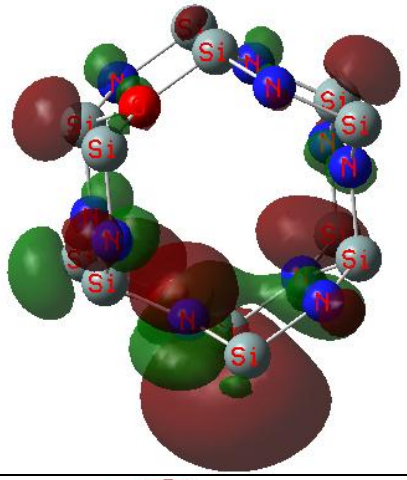	3.01	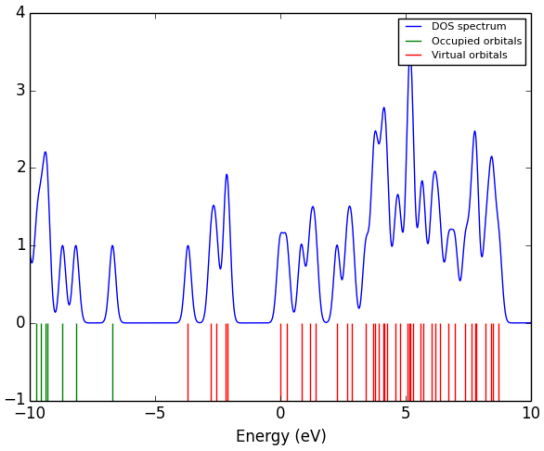
Ge substituted β-Si_3N_4 nanostructure	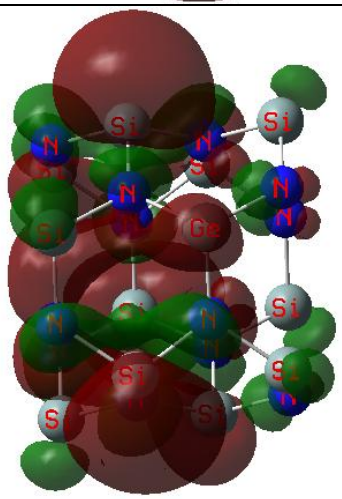	6.17	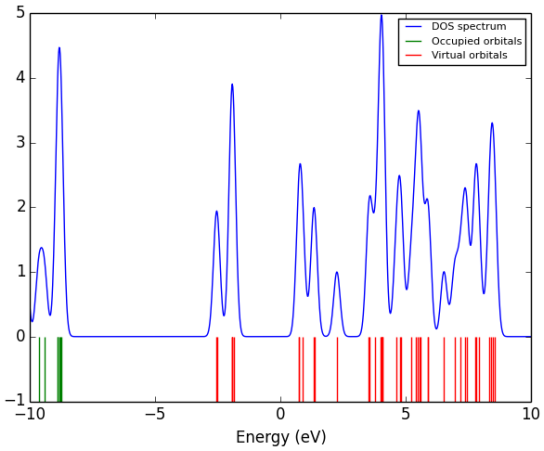

Defect structured β-Si_3N_4 nanostructure	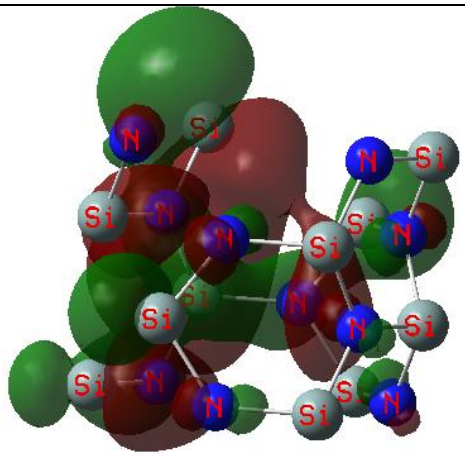	3.82	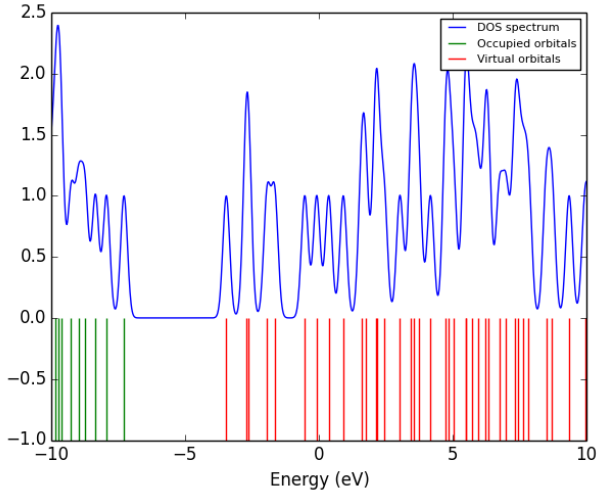

The visualization of HOMO – LUMO clearly represents the electron cloud in occupied and virtual orbital. The green color cloud shows the HOMO and red color shows the LUMO electrons in Si_3N_4 nanostructures. Surprisingly, on observing DOS spectrum, the charge density is low in occupied orbital and high in virtual orbital for pure, O and Ge substituted Si_3N_4 nanostructures. This refers the localization of charges along the virtual orbitals than in occupied orbitals. The overlapping of Si and N orbitals leads to localization of charges in virtual orbitals. Since the electronic configuration of Si is *[Ne]* $3s^2\ 3p^2$ and N is $1s^2\ 2s^2\ 2p^3$, when they overlap it gives rise to localization of charges along the virtual orbital [38, 39].

Ionization potential and electron affinity of Si_3N_4 nanostructures

The electronic properties of Si_3N_4 nanostructures can also be described in terms of electron affinity (EA) and ionization potential (IP) [40, 41]. The graphical representation of EA and IP of Si_3N_4 nanostructures are shown in Figure 2. The amount of energy needed to detach an electron from Si_3N_4 nanostructure is known as IP. The amount of energy released during the addition of electrons in Si_3N_4 nanostructures is known as EA. Almost same IP values are observed for all possible α-Si_3N_4 and β-Si_3N_4 nanostructures within the range of 8.13 – 8.78 eV, except for O substituted and defect structured β-Si_3N_4 nanostructures and the corresponding values are 6.69 and 7.28 eV respectively. Therefore, comparatively more energies are required for detaching the electron from Si_3N_4 nanostructures rather than O substituted and defect structures β-Si_3N_4 nanostructures. EA play a vital role in chemical sensors and plasma physics. Approximately same values of the EA are observed for Si_3N_4 nanostructures within the range of 2.56 – 3.68 eV. It implies that the moderately small amount of energies is released due to addition of electrons in Si_3N_4 nanostructures.

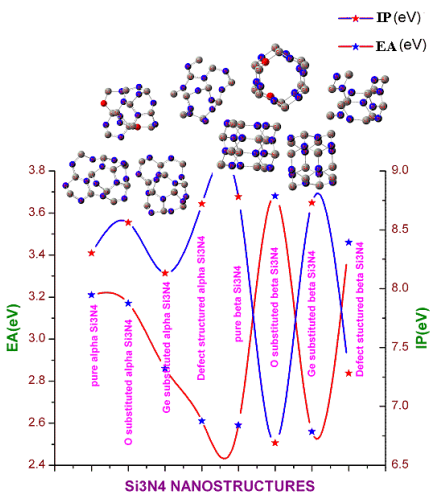

Figure. 2 IP and EA of Si_3N_4 nanostructures

Conclusions

With the help of DFT method, the realistic structures of pure, Ge and O substituted Si_3N_4 nanostructures are optimized and simulated successfully using B3LYP/LanL2DZ basis set. The structural stability of α-Si_3N_4 and β-Si_3N_4 are discussed in terms of calculated energy. The electronic properties of α-Si_3N_4 and β-Si_3N_4 are studied with HOMO-LUMO gap, DOS spectrum, electron affinity and ionization potential. Dipole moment and point symmetry of α-Si_3N_4 and β-Si_3N_4 are also reported. The present work provides insight on the structural stability and electronic properties of α-Si_3N_4 and β-Si_3N_4 with substitution impurity and defect in the nanostructure. Moreover, the structural stability and electronic properties of Si_3N_4 nanostructures can be enhanced with proper substitution impurity and creating defect in the nanostructure, which find its importance in cutting tools, engine components and microelectronic devices.

References

1. Katz R.N., High-Temperature Structural Ceramics, Science, 1980, 208, 841-847.
2. Liu A.Y. and Cohen M.L., Structural properties and electronic structure of low-compressibility materials: β-Si3N4 and hypothetical β-C3N4, Phys.Rev.B, 1990, 41, 10727.
3. Powell M.J, Easton B.C and Hill O.F., Amorphous silicon-silicon nitride thin-film transistors, Appl.Phys.Lett., 1981, 38, 794.
4. Riley F.L., Silicon nitride and related materials, J. Am. Ceram. Soc., 2000, 83, 245–265.
5. Xu X, Nishimura T, Hirosaki N, Xie R.J, Yamamoto Y and Tanaka H., Superplastic deformation of nano-sized silicon nitride ceramics, Acta Mater, 2006, 54, 255–262.
6. Reis P, Davim J.P, Xu X and Ferreira J.M., Friction and wear behaviour ofβ-silicon nitride-steel couples under unlubricated conditions, Mater. Sci. Technol., 2006, 22, 247–252.
7. Xu X, Nishimura T, Hirosaki N, Xie R.J and Tanaka H., Fabrication of a nanoSi3N4/nano-C composite by high-energy ball milling and spark plasma sintering, J. Am. Ceram. Soc., 2007, 90, 1058–1062.
8. Xu X, Nishimura T, Hirosaki N, Xie R.J, Zhu Y.C and Yamamoto Y., New strategies to preparing nano-sized silicon nitride ceramics, J. Am. Ceram. Soc., 2005, 88, 934–937.
9. Atkinson A, Moulson A. J and Roberts E. W., Nitridation of high-purity silicon, J Am Ceram Soc, 1976, 59, 285-289.
10. Licko T, Figusch V and Puchyova J., Synthesis of silicon nitride by carbothermal reduction and nitriding of silica: Control of kinetics and morphology, J Eur Ceram Soc, 1992, 9, 219-230.
11. Petzow G and Herrmann M., Silicon nitride ceramics: Structure and Bonding, Springer-Verlag Berlin Heidelberg, 2002, 102, 50-167.
12. Nakamura M, Kuranari Y and Imamura Y., Characterization and synthetic process of Si3N4material powder. In: S. Somiya, et al., Silicon nitride 1. Elsevier, London, 1987, 40.
13. Bauer J., Optical properties, band gap, and surface roughness of Si3N4, Phys. Stat. Sol. A, 1977, 39, 411- 418.
14. Gritsenko V.A, Shaposhnikov A.V, Kwok W.M, Wong H and Jidomirov G.M., Valence band offset at silicon/silicon nitride and silicon nitride/silicon oxide interfaces, Thin Solid Films, 2003, 437, 135 - 139.
15. Pic N, Glachant A, Nitsche S, Hoarau J.Y, Goguenheim D, Vuillaume D, Sibai A and Chaneliere C., Determination of the electrical properties of ultrathin silicon-based dielectric films: thermally grown SiN_x, Solid-State Electron, 2001, 45, 1265-1270.
16. Bermudez V.M., Theoretical study of the electronic structure of the Si3N4(0 0 0 1) surface, Surface Science, 2005, 579, 11–20.
17. Aberle A.G and Hezel R., Progress in low-temperature surface passivation of silicon solar cells using remote-plasma silicon nitride, Prog. Photovoltaics, 1997,5, 29–50.
18. Nagel H, Aberle A.G and Hezel R., Optimised antireflection coatings for planar silicon solar cells using remote PECVD silicon nitride and porous silicon dioxide, Prog. Photovoltaics, 1999, 7, 245–260.
19. Parm I.O, Kim K, Lim D.G, Lee J.H, Heo J.H, Kim J, Kim D.S, Lee S.H and Yi J., High-density inductively coupled plasma chemical vapor deposition of silicon nitride for solar cell application, Sol. Energy Mater. Sol. Cells, 2002, 74, 97–105.
20. Soppe W, Rieffe H and Weeber A., Bulk and surface passivation of silicon solar cells accomplished by silicon nitride deposited on industrial scale by microwave PECVD', Prog. Photovoltaics, 2005, 13, 551–569.
21. Verlaan V, van der Werf C.H.M, Flouweling Z.S, Romijn G, Weeber A.W, Dekkers H.F.W, Goldbach H.D and Schrop R.E.I., Multi-crystalline si solar cells with very fast deposited (108 nm/min)

passivating hot wire CVD silicon nitride as antireflection coating', Prog. Photovoltaics, 2007, 15, 563–573.

22. Yoo J.S, Dhungel S.K and Yi J.S., Annealing optimization of silicon nitride film for solar cell application, Thin Solid Films, 2007, 515, 7611–7614.
23. Pliskin W.A., The evaluation of thin film insulators, Thin Solid Films, 1968, 2, 1 - 2.
24. Yang P, Fun H.-K, Rahman I.A and Saleh M.I., Two phase refinements of the structures of α-Si_3N_4 and β-Si_3N_4 made from rice husk by Rietveld analysis , Ceram.Int., 1995, 21, 137 - 142.
25. Wang C.M, Pan X.Q, Ruhle M, Riley F.L and Mitomo M., Silicon nitride crystal structure and observations of lattice defects , J.Mater.Sci., 1996, 31, 5281 - 5298.
26. Toraya H., Crystal structure refinement of α-Si_3N_4 using synchrotron radiation powder diffraction data: unbiased refinement strategy, J.Appl.Cryst., 2000, 33, 95 - 102.
27. Wang X.-s., Zhai G, Yang J and Cue N., Crystalline Si3N4 thin films on Si(111) and the 4×4 reconstruction on Si3N4(0001), Phys.Rev.B, 1999, 60, R2146.
28. Zhai G, Yang J, Cue N and Wang X.-s., Surface structures of silicon nitride thin films on Si(111), Thin Solid Films, 2000, 366, 121 - 128.
29. Chandiramouli R, Sriram S and Balamurugan D., Quantum chemical studies on (ZnO) n/(NiO) n heterostructured nanoclusters, Moecular Physics, 2014, 112, 151-164.
30. Sriram S and Chandiramouli R., A study on the electronic properties of GaInPAs nanostructures: A density functional theory approach, The European Physical Journal Plus, 2013, 128, 1-8.
31. Chandiramouli R. A DFT study on the structural and electronic properties of Barium Sulfide nanoclusters, Research Journal of Chemical Environment, 2013, 17, 64-73.
32. Frisch M. J, Trucks G. W, Schlegel H. B, Scuseria G. E, Robb M. A, Cheeseman J. R, Scalmani G, Barone V, Mennucci B, Petersson G. A, Nakatsuji H, Caricato M, Li X, Hratchian H. P, Izmaylov A. F, Bloino J, Zheng G, Sonnenberg J. L, Hada M, Ehara M, Toyota K, Fukuda R, Hasegawa J, Ishida M, Nakajima T, Honda Y, Kitao O, Nakai H, Vreven T, Montgomery J A, Jr., Peralta J. E, Ogliaro F, Bearpark M, Heyd J. J, Brothers E, Kudin K. N, Staroverov V. N, Kobayashi R, Normand J, Raghavachari K, Rendell A, Burant J. C, Iyengar S. S, Tomasi J, Cossi M, Rega N, Millam N. J, Klene M, Knox J. E, Cross J. B, Bakken V, Adamo C, Jaramillo J, Gomperts R, Stratmann R. E, Yazyev O, Austin A. J, Cammi R, Pomelli C, Ochterski J. W, Martin R. L, Morokuma K, Zakrzewski V. G, Voth G. A, Salvador P, Dannenberg J. J, Dapprich S, Daniels A. D, Farkas Ö, Foresman J. B, Ortiz J. V, Cioslowski J and Fox D. J., Gaussian, Inc., Wallingford CT, Gaussian 09 Revision D.01 2009.
33. Becke A.D., Density-functional exchange-energy approximation with correct asymptotic behavior, Physical Review A, 1988, 38, 3098 .
34. Becke A.D. Density-functional thermochemistry. III. The role of exact exchange, Journal of Chemical Physics, 1993, 98, 1372.
35. O'Boyle N. M, Tenderholt A. L and Langner K. M., GaussSum Version 3.0, Journal of Computational Chemistry, 2008, 29, 839-845.
36. Nagarajan V and Chandiramouli R., Effect on the structural stability and electronic properties of impurity substituted sodium selenide nanostructures – A quantum chemical study, Int.J. ChemTech Res., 2014,6(4), 2240-2246.
37. Sriram S, Chandiramouli R, Balamurugan D and Thayumanvan A., A DFT study on the structural and electronic properties of ZnTe nanoclusters, European Physical Journal of Applied Physics, 2013, 62, 30101.
38. Nagarajan V and Chandiramouli R., Quantum Chemical Studies on ZrN Nanostructures, Research journal of pharmaceutical biological and chemical sciences, 2014, 6 (1). 21-30.
39. Nagarajan V and Chandiramouli R., Investigation on the structural stability and electronic properties of InSb nanostructures–A DFT approach, Alexandria Engineering Journal, 2014, 53 (2), 437-444.
40. Nagarajan V and Chandiramouli R., A quantum chemical exploration on structural stability and electronic properties of CdZnO nanostructures, Der Pharma Chemica., 2014, 6 (1), 37-46.
41. Nagarajan V and Chandiramouli R., Exploring structural stability and electronic properties of SnSe nanostructures-A DFT study, Der Pharma Chemica., 2014, 6(2), 239-251.

*****